JOURNAL OF GEOPHYSICAL RESEARCH, VOL. 99, NO. C8, PAGES 16,341–16,350, AUGUST 15, 1994

Surface characteristics of lead ice

Donald K. Perovich and Jacqueline A. Richter-Menge
U.S. Army Cold Regions Research and Engineering Laboratory, Hanover, New Hampshire

Abstract. Under cold conditions, ice growth in a lead occurs rapidly, giving young sea ice a high bulk salinity. The surface characteristics of this ice type are dominated by a thin, highly saline surface skim and often by the formation of frost flowers. These surface characteristics are of particular interest because of their significant temporal variability and large impact on the electromagnetic properties of sea ice. As part of the Lead Experiment held during March and April of 1991 and 1992 in the Alaskan Beaufort Sea, ice properties and surface conditions typical of springtime leads were monitored at three sites during the initial few days of growth. Observations indicate that once the ice thickness reached approximately 2 cm, a thin (~1 mm), highly saline (~100 parts per thousand (ppt)) skim of brine formed on the surface. After only a few hours of growth the initially smooth surface of the sea ice developed some small-scale roughness. Frost flowers, the result of ice grown from the vapor phase, quickly formed on the surface of the sea ice and continued to develop during the observations. Depending on the temperature, the frost flowers were composed of various ice crystal types, including clumps, stellar dendrites, and needles. The initially fresh frost flowers quickly became salty, reaching salinities as high as 100 ppt. The salinity of both the frost flowers and the surface skim decreased at night as temperatures dropped and additional hoarfrost accumulated on the surface. These decreases were also due in part to the accumulation of snow on the surface of the leads. Combining these observations with simple calculations, possible mechanisms for the development and evolution of the surface skim and frost flowers are discussed. They include the hypothesis that the source of the surface skim is brine expelled upward from the sea ice as it cools, that the surface protrusions serve as nucleation sites for the frost flowers, and that the source of the excess water vapor necessary for frost flower growth is the wet surface skim.

Introduction

The Arctic ice pack is extremely dynamic, undergoing periods of convergence and divergence in response to winds and ocean currents. The development of leads is an important consequence of this continual motion. Leads are linear breaks in the sea ice cover that typically open to widths of tens to hundreds of meters, exposing the relatively warm underlying ocean water to the cold air. In these areas of open water, heat loss to the atmosphere reaches a maximum and results in the rapid growth of ice. Theoretical studies [*Maykut*, 1982] have established the importance of this period of young ice growth in leads to basinwide ice production, atmospheric heat fluxes, and salt input to the upper ocean. The relatively thin ice also plays a critical role in controlling the large-scale strength and dynamic behavior of the ice pack.

Field and laboratory observations and measurements consistently indicate that during the initial hours of new sea ice growth, a liquidlike skim develops on the surface of the ice. This surface or brine skim is approximately 1 mm thick and, as reported by *Drinkwater and Crocker* [1988], often has a salinity in excess of 100 parts per thousand (ppt). If wind conditions are light, so-called frost flowers, which have a bulk salinity comparable to the surface skim, often form on the new sea ice as it begins to thicken. Generally, within several days these surface conditions have been significantly modified. This is mainly due to the fact that the frost flowers are extremely effective collectors of blowing snow and, as a consequence, are quickly covered. As snow accumulates, the brine that forms the surface skim and exists in the frost flowers is drawn into the snowpack, reducing the overall salinity. For instance, *Crocker and Lewis* [1985] observed that approximately 3 weeks after a sea ice cover had initially formed over a lead, the salinity of the surface layer decreased from 105 to 50 ppt.

Reports of the presence of a surface skim and frost flowers are most abundant in the journals of early Arctic and Antarctic explorers and scientists [*Drinkwater and Crocker*, 1988]. More recently, attention has again been focused on this phenomenon, since it appears to have a significant impact on the electromagnetic properties of sea ice, affecting its remote-sensing signature. For instance, *Wensnahan et al.* [1993] present data on the microwave emission of young, saline ice, illustrating temporal variations in brightness temperature over a range of frequencies as the ice thickness increased from 0 to 9 cm. In the case of sea ice grown artificially in the laboratory, they observed a significant decrease in the brightness temperature at higher frequencies when the ice was between 1 and 2 cm thick, rather than the monotonic rise that would be expected on the basis of an assumption that the ice uniformly cools as it thickens. In fact, they found a rapid increase in the surface temperature

Paper number 94JC01194.

of the ice sheet of several degrees associated with the decrease in brightness temperature. On the basis of physical observations, they suggest that this is a result of the upward transport of warm brine from the interior of the sea ice to the surface. Similarly, active microwave backscatter measurements exhibit a distinctive variability during the early period of sea ice growth. Measurements at C and X bands show that a minimum in the backscattering coefficient occurs when the sea ice is about 2 cm thick due to the increase in salinity on the surface of the ice [*Grenfell et al.*, 1993; *Onstott*, 1993]. This is followed by a strong maximum that coincides with the formation of frost flowers. It remains unclear, however, whether this maximum reflects changes in the dielectric properties of the sea ice or its surface roughness. The growth of frost flowers also causes the albedo of the newly forming sea ice cover to increase, influencing the thermodynamics of the ice and the underlying water column.

While there has been a significant amount of speculation concerning the formation of the highly saline surface skim and frost flowers, little progress has been made in measuring their physical properties and investigating the physical processes involved. We had the opportunity to address this issue as part of our research activities in the Lead Experiment (LEADEX) held during April in 1991 and 1992 in the Alaskan Beaufort Sea [*LEADEX Group*, 1993]. During both phases of the field program the formation of a surface skim and frost flowers on newly forming sea ice was pervasive. This observation, combined with those of earlier investigators, confirms that these features are characteristic of sea ice growth under springtime conditions when there are significant amounts of incident solar radiation but air temperatures remain low. More detailed observations of the temporal variations in the surface properties of the young sea ice and the associated environmental conditions were made at three leads. This paper presents the results of the studies we conducted at each location and couples them with other concurrently measured physical property data in an effort to gain insight into the mechanisms involved in the development of lead ice surface features.

Field Experiment

The overall objective of the LEADEX program was to develop a better understanding of the processes of heat transfer to the atmosphere and salt rejection to the underlying ocean that occur during the initial ice growth on a newly opened lead. The associated field experiment was designed to allow for the rapid deployment of investigators from a base camp, located approximately 250 km north of Prudhoe Bay, Alaska, to the site of an open lead within hours of its formation. Once on site, investigators installed their equipment and made measurements during freeze-up. In April 1991 a pilot study was conducted that focused on working out the complicated logistics involved in moving personnel and their living and scientific gear to the lead site. Fortunately, there was a significant amount of ice movement near the base camp, which resulted in the formation of numerous leads, affording the opportunity to make initial scientific observations. In the main field program, held the following year, four lead sites were investigated over the course of a 5-week operations window in late March and April. These remote camps lasted from 2 to 4 days, depending on the dynamics of the lead. During this period there was a transition from open water to an ice cover that was 15 to 25 cm thick.

Our efforts in the field program specifically focused on monitoring the temporal variations in ice surface conditions and in the physical properties of the newly forming ice. Detailed measurements of the physical properties of the sea ice surface were made at three different leads: one during the pilot study (April 14–20, 1991) and two during the main field experiment (April 6–9 and April 11–14, 1992). The latter are referred to as leads 3 and 4, respectively, by participants in the LEADEX program [*LEADEX Group*, 1993]. Casual observations made at a number of other nearby leads indicated that these leads were indeed representative examples of ice conditions and growth processes taking place in the vicinity of the LEADEX camp. Environmental conditions were similar at all of the leads observed: air temperatures between −25°C and −15°C, light winds, high relative humidity (85–95%), and significant amounts of incident solar radiation (peak values near 450 m^{-2} and daily averages of 150 W m^{-2}). Since high winds prevented the helicopter operations necessary to establish lead camps, we do not have observations of lead ice surface conditions during high winds. In all the cases observed, ice growth began under quiescent conditions, with only a small amount of frazil ice production. Deformation of the newly formed lead ice was common, resulting in both rafting of the lead ice and reopening of the lead.

In the pilot phase the one lead site we investigated was within walking distance of the base camp, permitting us to make observations and measurements for a continuous 6-day period. This included measurements of vertical profiles of sea ice temperature, salinity, and structure on 105-mm-diameter cores removed from the growing ice sheet. Ice temperatures were measured as soon as the core was pulled from the ice sheet by inserting a digital thermometer probe into holes drilled into the side of the core at intervals of 0.05–0.10 m. These temperature measurements were made with an estimated accuracy of ±0.1°C. After the vertical temperature profile of the ice core was determined, the core was cut into 0.02- to 0.10-m-long pieces which were melted in a closed container for salinity measurements. Salinities were determined from conductivities measured on a Beckman Solubridge that had been calibrated against solutions prepared from Copenhagen standard seawater. All salinities were corrected to a reference temperature of 25°C. Measurement precision is estimated at ±0.2 ppt. A second core was taken to determine the crystalline structure of the ice. This core was placed in a tube, boxed in an insulated container that was charged with dry ice, and shipped back to the Cold Regions Research and Engineering Laboratory (CRREL) in Hanover, New Hampshire, for analysis. The continuous vertical profile of the ice structure was identified by studying thin sections placed between crossed polaroids [*Gow et al.*, 1987]. Horizontal thin sections were also made at selected locations in the core, usually marking a change in crystal type.

In the course of monitoring the lead in the pilot study and observing others in the area, it became evident that the development of a surface brine skim and frost flowers on young sea ice was commonplace and was a normal step in the formation of sea ice under springtime conditions. Photographs were taken to document the changes in the surface conditions of the sea ice, along with coincident measurements of the air and ice surface temperatures. Isolated salinity measurements were also made of the surface skim and the frost flowers. Using these observations as a foundation, our ice core sampling procedures were augmented in the main experiment with a more rigorous set of measurements to determine the temporal variations in the salinity of the frost flowers and surface skim.

Specifically, at lead 4 we made a detailed time series of the salinity of the sea ice, brine skim, and frost flowers. Ice cores were analyzed to determine the salinity profile at 1-cm intervals of the upper portion of the sea ice. In addition, the surface skim and the frost flowers were sampled independently from the sea ice. Given the low density of the frost flowers, we chose to obtain a salinity sample by clearing a group of frost flowers from the surface of the sea ice, rather than attempting to measure them individually. Frost flowers were harvested from an area of roughly 200 cm^2 to generate each sample. The frost flowers were collected by using a flat metal spatula to first carefully remove the top half of the frost flowers followed by the bottom half, placing each layer in a separate container. Once the frost flowers were removed, the underlying surface skim was then sampled, again using the spatula. The frost flower and surface skim samples were melted in a closed container, and because of their small size, salinity was measured using an optical salinometer. The salinometer had an accuracy of 1 ppt, though actual uncertainties are larger because of the intrinsic spatial variability of sea ice salinity [*Tucker et al.*, 1989], difficulties in sampling the frost flowers, and the limited number of samples. We estimate uncertainties of approximately ±5 ppt in salinity for the frost flowers and brine skim. Temperature measurements of the surface brine skim were made using the digital thermometer probe described earlier. The thickness of the brine layer and the height of the frost flowers were measured using a millimeter-scale ruler. Therefore the measured thickness of the brine skim can only be considered an estimate with a typical value of 1–2 mm ± 1 mm.

Observations

As we have described, when a lead opens in the ice pack during winter and spring, relatively warm ocean water is exposed to cold air. Under these conditions, ice growth can be very rapid. For example, ice growth due to heat conduction at an average air temperature of −20°C can produce a sea ice cover that is 20 cm thick in less than 2 days. The specific nature of the initial ice growth depends on the environmental conditions [*Weeks and Ackley*, 1982]. Under turbulent conditions a slurry consisting of granular ice and brine forms and consolidates. If conditions are quiescent, a thin, granular surface layer develops that quickly evolves into a columnar transition zone with intracrystalline ice platelets growing downward into the supercooled water. In both cases, ice growth is so rapid that most of the salts in the water are trapped within the sea ice, creating high salinities in the top few centimeters of the ice sheet.

In the three leads we studied, ice growth occurred under quiescent conditions, beginning with a thin ice layer that formed almost immediately after the lead opened. Structurally, the upper portion of the sea ice consisted of a 5-mm-thick granular layer transitioning to columnar ice below. By the time we arrived at the lead sites, the ice had already reached a thickness of several centimeters and a brine skim, approximately 1–2 mm thick, had developed on the surface. The brine skim persisted over the next few days as the ice grew to a thickness of 0.2 m. During this period the once flat ice surface developed some small-scale topography, with roughness elements on the order of a few millimeters high and tens of millimeters across.

As the lead ice continued to grow, small crystals, called frost flowers, began to appear on the surface. For example, Figure 1 shows ice conditions 3 hours after the lead opened at the main experiment's lead 4 site. A sparse distribution of frost flowers is apparent on the ice cover, which had grown to a thickness of 3 cm and had developed a brine skim. The white area in the foreground of the photograph is where snow had drifted onto the lead ice. A narrow band of open water is also visible in the background. As time progressed, more frost flowers formed, making the covering denser.

From an oblique angle, frost flowers appear to cover the lead ice in a continuous white blanket, as shown in Figure 2a, which illustrates conditions 48 hours after the lead opened during the pilot study. If the surface is examined more closely, looking directly downward (Figure 2b), it is apparent that the frost flowers do not cover the sea ice uniformly, but rather are discrete clumps of ice crystals. In this particular case the frost flowers covered only one third of the surface area, and the clumps were composed of aggregated fine stellar dendrite crystals. These frost flowers formed under relatively warm conditions; the air temperature was −12°C, and the ice surface temperature was −6°C when the photographs were taken.

Image processing techniques were used to examine the size, shape, and distribution of the clumps in Figure 2b in an effort to quantify the frost flower coverage. Individual clumps had a roughly circular shape, though in many places they had merged to form elongated structures. The clumps were on the order of 1 cm high and had cross-sectional areas ranging from 2 to 148 cm^2 and averaging 16 cm^2. The average length of the major axes of the clumps was 5.6 cm, with a range from 1.6 cm to 36 cm. The maximum length corresponded to the long, narrow conglomeration of clumps down the right-hand side of Figure 2b.

The specific crystal form or habit that the frost flowers take depends on the growth conditions. We observed two distinct crystal types, in addition to those shown in Figure 2, which grew at different temperatures (Figure 3). Note that in Figures 3a and 3b the surface brine skim is clearly evident as a bright sheen between the frost flowers. Fanlike stellar dendrites developed at a lower air temperature of −16°C (Figure 3a). These crystals were extremely thin and grew as large as 2.5 cm high and 1.5 cm wide. At an even lower air temperature of −22°C the crystals were again quite different, with 2- to 3-cm-long needlelike crystals forming (Figure 3b).

As was stated earlier, frost flowers formed rapidly. They can also disappear rapidly. This was particularly evident during periods of surface flooding, which occurred frequently because the thin lead ice deformed easily. Even a small amount of surface flooding was sufficient to melt any frost flowers that were present. More subtle changes in the characteristics of the frost flowers were occurring almost continuously. For example, we observed small diurnal changes in the form of the frost flowers at all three lead sites. During the course of the day, as air temperatures increased, the flowers deteriorated, losing much of their dendritic structure. As temperatures dropped in the evening and night,

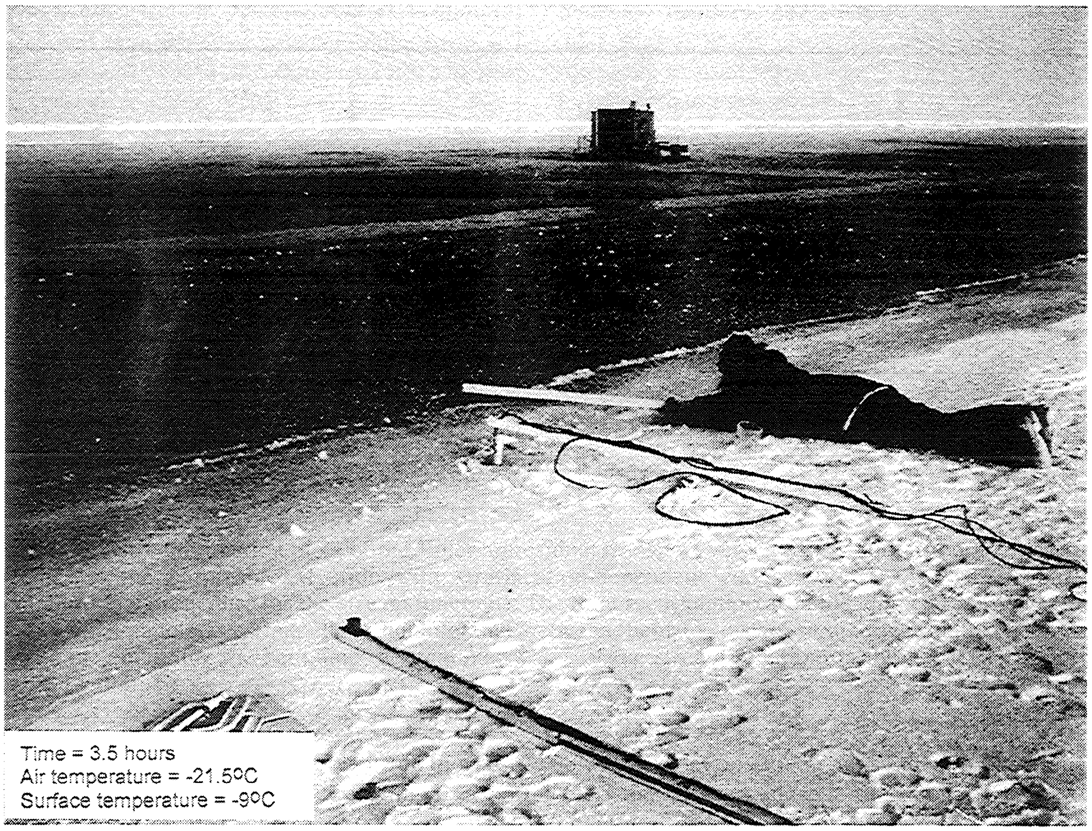

Figure 1. Frost flowers beginning to form on lead 4 in the main experiment 3 hours after the lead opened. The air temperature was −22°C.

growth began again on the existing flowers. With its wet surface skim and the rough protuberances of the frost flowers, the "sticky" surface of the lead ice was an efficient collector of blowing snow. This resulted in the obscuration and burial of the frost flowers under a layer of snow, which has been observed to occur within several days of their initial formation [*Crocker and Lewis*, 1985].

The salinity and brine volume of the surface of the sea ice is important because of its large impact on microwave signatures. The temporal evolution of salinity in the ice, surface skim, and frost flowers over the first few days of ice growth in lead 4 of the main experiment is illustrated in Figure 4. As described earlier, the frost flowers were sampled in two segments: the top and the bottom. The most striking feature is the high salinity of the surface skim and the base of the frost flowers, which was on the order of 100 ppt. Salinities in the top portion of the frost flowers were consistently 30 ppt lower than in the base. Salinities in the base of the frost flowers were slightly higher and well correlated with those in the brine skim. Over the course of 2 days the salinity of the surface skim and frost flowers increased at first, reached a peak, and then began to drop. Salinities decreased as additional ice formed on the frost flowers and as small amounts of windblown snow accreted on the wet, sticky ice surface. Using a temperature of −20°C, salinity of 100 ppt, and a pure ice density of 0.920 g cm^{-3} and the brine volume relationship of *Cox and Weeks* [1983], we determined that by volume, the frost flowers were composed of approximately three parts ice and one part brine. This brine volume is slightly lower than that of the surface skim, primarily because of the lower temperature of the frost flowers. Unfortunately, we do not have microscale observations of how this brine was distributed upon individual frost flowers.

The total volume of brine present in the upper portion of the sea ice, the surface skim, and the frost flowers was also examined. Using the observed temperatures and salinities and assuming that the frost flowers and sea ice had densities of 0.025 g cm^{-3} and 0.920 g cm^{-3}, respectively, we again applied the brine volume equations developed by Cox and Weeks. The results, shown in Figure 5, demonstrate that even though the salinity of the frost flowers was comparable to the salinity of the surface skim, their total brine content was more than an order of magnitude smaller. The total brine content of the surface skim was typically in the range of 250–400 cm^3 L^{-1}, while the frost flowers had a total brine content of the order of 10 cm^3 L^{-1}, less than 5% of the surface skim brine content.

Discussion

Brine Skim

A number of researchers have attributed the formation of the surface skim to an upward expulsion of brine that occurs in the top portion of the sea ice sheet during cooling [*Drinkwater and Crocker*, 1988; *Grenfell and Comiso*, 1986]. The measurements of *Wensnahan et al.* [1993] further note that this brine skim does not appear until the sea ice is 1 to 2 cm thick. While the presence of a surface brine skim is well documented, its origin is still a matter of some conjecture.

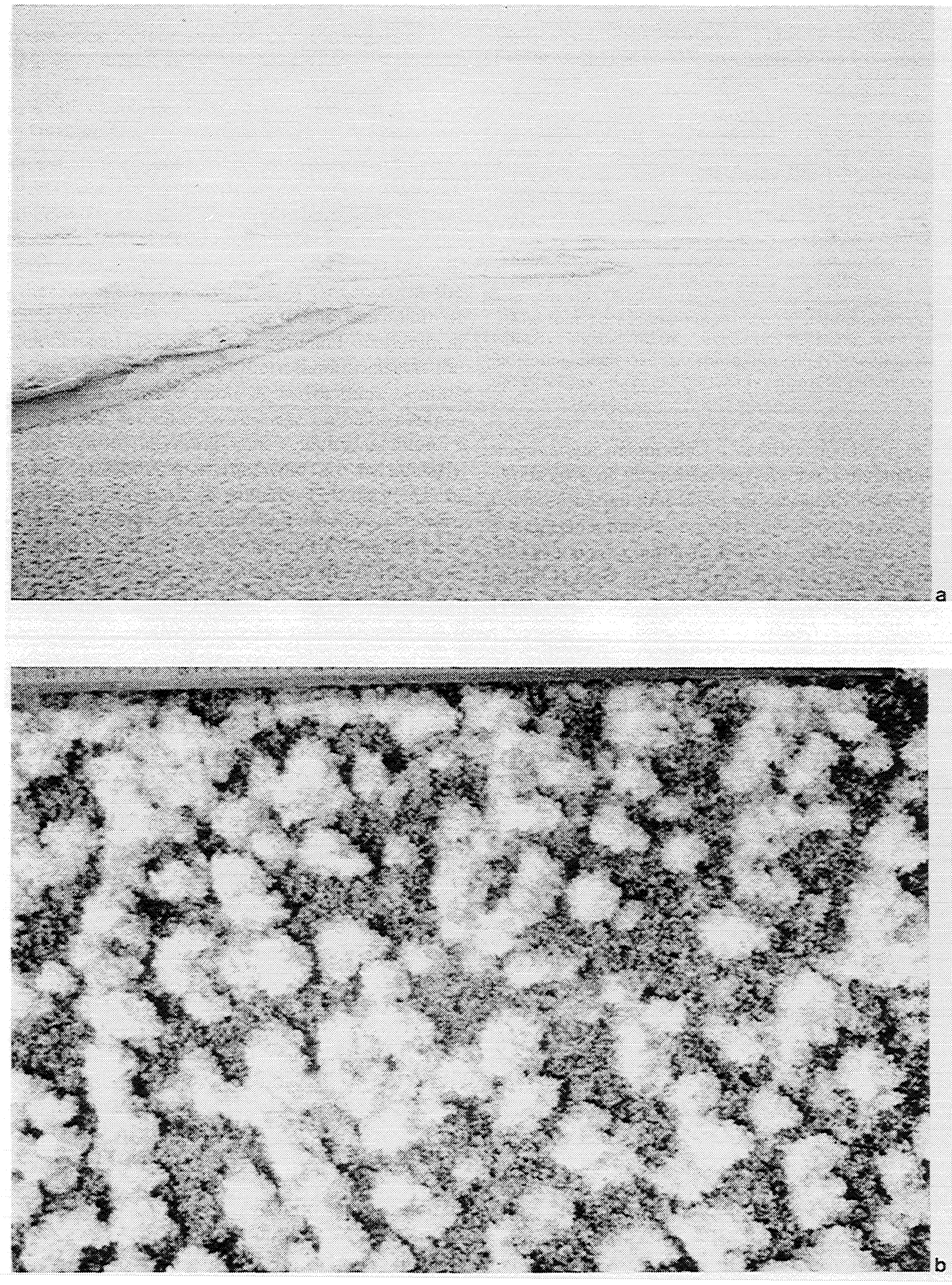

Figure 2. Frost flower conditions 48 hours after the lead investigated during the pilot study opened: (a) from an oblique angle where the frost flowers appear to cover the sea ice in a continuous white blanket and (b) looking directly downward, where it is apparent that the frost flowers did not form a continuous blanket, but rather were discrete clumps of ice crystals.

Ono and Kasai [1985] speculated that the highly saline surface skim resulted from upward brine seepage through porous ice due to the relative depression of the ice cover.

Our observations and measurements, which show an initial increase in the salinity of both the surface skim and the frost flowers, support the conjecture that the source of the surface skim is brine rejected from the upper portion of the sea ice during cooling. At the lead sites we investigated, the first centimeter of ice grew very quickly and ice salinities were high, near 30 ppt, in agreement with the detailed laboratory observations of *Cox and Weeks* [1975]. These high salinities indicate that large amounts of brine have been trapped in the sea ice. During the rapid initial growth, there was little cooling of the sea ice. As the sea ice grew thicker,

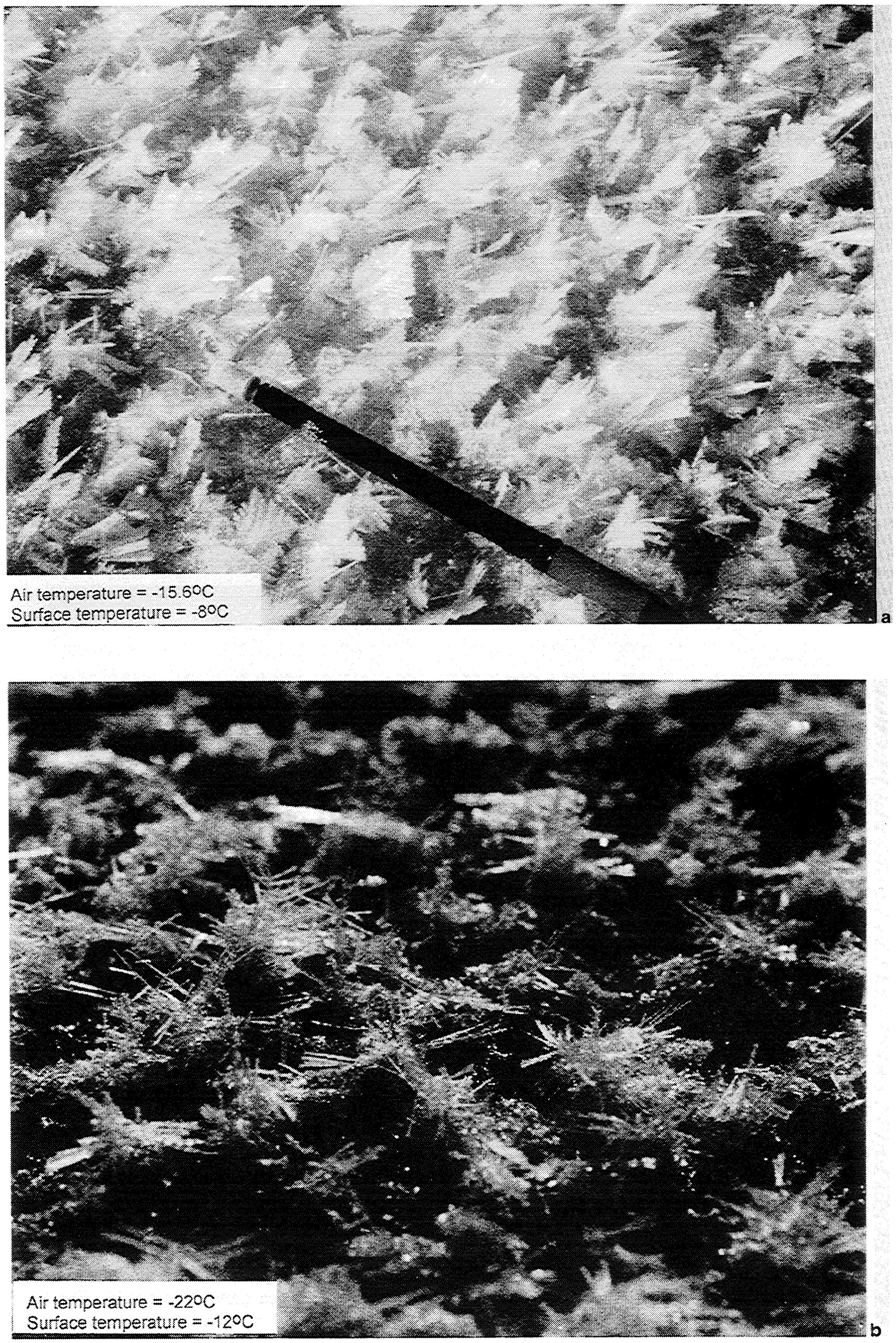

Figure 3. Observed crystal forms of frost flowers: (a) stellar dendrites grown at an air temperature of −16°C and (b) long needles grown at −22°C.

cooling began. When the ice cools, some of the trapped brine freezes, increasing its volume and causing some brine to be expelled. The young sea ice has a large bulk porosity and a complex internal structure, which near the surface includes multiple ice platelets at a variety of orientations surrounded by numerous air and brine inclusions. Detailed brine volume profiles of young, thin sea ice [*Cox and Weeks*, 1975] indicate that porosities are large near the surface, decreasing to minimum values a few centimeters below the surface, and then increasing again at greater depths. We would expect the permittivity of this structurally homogeneous young ice to be correlated with its porosity. This is supported by the work of *Ono and Kasai* [1985], who determined in laboratory experiments that in young sea ice the upward permeability was greater than the downward permeability and that the upward-to-downward ratio increased as the sea ice cooled. This vertical distribution of porosity, and in all likelihood permeability, facilitates the upward movement of some of the expelled brine, even though the sea ice is cooling from the surface, and therefore could contribute to the development of the highly saline surface skim. Continued cooling of the sea ice would result in more rejected brine, thereby augmenting the brine skim. A relevant analogy is to think of the young ice, with its high porosity and brine volume, as a sponge. Expansion resulting from freezing of the included brine during cooling then has the effect of squeezing the sponge, expelling brine to the surface.

Using the LEADEX measurements, we can quantitatively evaluate the plausibility of this scenario. Specifically, by assuming a constant sea ice density of 920 kg m^{-3}, we can estimate the thickness of the ice layer (H) that must contribute brine to the surface skim in order to achieve the high salinities we measured. The mass of salt per unit area contained in the brine skim (M_{bs}) is the product of the density (1080 kg m^{-3}), the salinity (100 g kg^{-1}), and the thickness (1 mm) of the brine skim and is roughly equal to 0.11 kg m^{-2}. The amount of salt in the brine expelled from the sea ice to the surface skim (M_i) is

$$M_i = f\rho_i(S - S_0)H \quad (1)$$

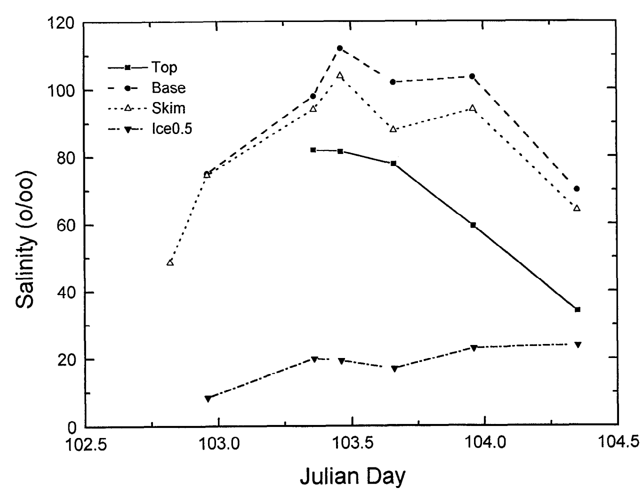

Figure 4. The temporal evolution of salinity in the sea ice, surface skim, and top and base of the frost flowers during the first few days of growth measured at lead 4 in the main experiment.

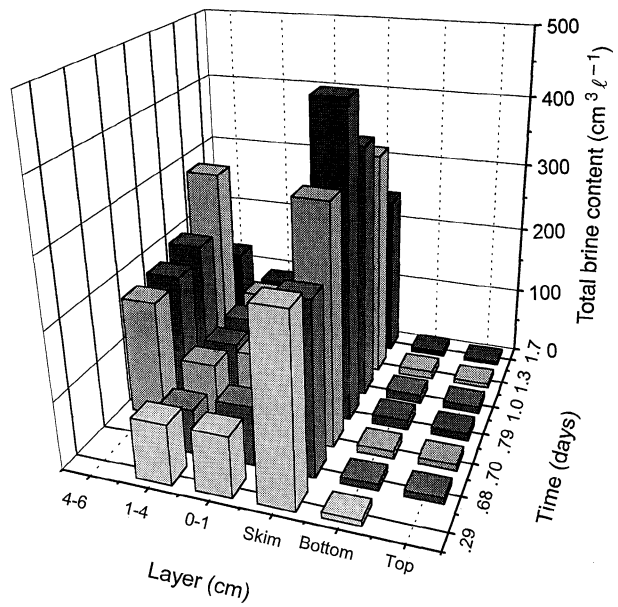

Figure 5. Volume of brine in frost flowers, surface skim, and upper portion of the sea ice cover as a function of time.

where f is the fraction of the brine that is expelled upward, ρ_i is the density of the sea ice, S_0 is the initial ice salinity, and S is the ice salinity after expulsion. If expulsion is the sole source of salt for the brine skim, then $M_i = M_{bs}$ and we can solve for H. The value of f is not known, so we shall make the simple assumption that half of the expelled brine goes upward to the surface and half goes downward (f = 0.5). S is determined using the relationship of *Untersteiner* [1968],

$$S = S_0(\theta_0/\theta)^{\Delta\rho/(1-\Delta\rho)}$$

where S_0 is the initial salinity, $\Delta\rho$ is the difference in density between brine and ice, and θ_0 and θ are the initial and final temperatures. Though this relationship was derived to investigate expulsion of brine downward in cooling ice, we believe that it is reasonable to apply it to upward expulsion in cooling ice as well. On the basis of our observations, S_0 = 30 ppt, $\Delta\rho = 0.1$, $\theta_0 = -2°C$, and $\theta = -15°C$, giving a final bulk salinity (S) of 24 ppt. Substituting these values into (1) gives $H = 0.04$ m. On the basis of porosity profiles of the upper portion of young sea ice, it seems reasonable that the top several centimeters of the sea ice could indeed contribute brine to the surface skim. Therefore while providing only an estimate, this analysis does support the premise that brine expelled from the upper portion of the sea ice is the source of the brine skim. Carefully controlled laboratory experiments, such as growing sea ice with a tracer in the brine, are still needed as a more definitive clarification of this issue.

The small-scale roughness that develops on the sea ice surface is also likely to be a direct consequence of the brine that is expelled upward to form the skim. When brine leaves the sea ice at the ice/water interface, rather than being rejected uniformly, it exits at discrete points that mark the locations of brine channels [*Weeks and Ackley*, 1982]. Similarly, we suggest that the brine expelled at the ice/air interface "erupts" at individual points on the surface. As the surface cools, some of the expelled brine must freeze to maintain equilibrium. In fact, we deduce that while the surface skim is wet, it is not exclusively composed of brine. Instead, it is a brine slurry that contains ice crystals. For example, using a measured surface skim salinity of 100 ppt and a surface temperature of $-15°C$ and assuming an ice density of 0.920 g cm^{-3}, according to the brine volume relationship of *Cox and Weeks* [1983] the surface skim is a mixture of 40% brine and 60% ice. Thus as the brine erupts onto the surface, it cools, forming ice crystals, which then consolidate, producing a small mound around the brine tube. As we will discuss in the next section, the development of this small-scale surface topography appears critical for the formation of frost flowers and may, by increasing surface scattering, affect the microwave signature of the sea ice.

Frost Flowers

In the past there has been some discussion about the origin of these surface crystals, in particular, whether they were frost flowers (ice grown from the vapor phase and therefore representing a form of surface hoar) or salt flowers (crystallized solid salts). We believe that all the flowers we observed during LEADEX were frost flowers and, for many reasons, that this is generally the case. This opinion is primarily based on the fact that the fabric of the observed crystals, and their temperature dependence, are consistent with the results of detailed studies on ice grown from the vapor phase [*Nakaya*, 1954; *Kobayashi*, 1961; *Magono and Lee*, 1966; *Hobbs*, 1974]. These studies have consistently shown that in ice grown from the vapor phase the crystal form depends primarily on the temperature and, to a lesser extent, the saturation. For example, *Magono and Lee* [1966] found stellar dendrites at vapor densities above water saturation and temperatures from $-13°$ to $-17°C$ and found needles at vapor densities between ice and water saturations and temperatures from $-20°$ to $-30°C$. In contrast, monoclinic crystals, with no temperature dependence, would be expected for salt flowers. Also, the primary salt in seawater, $NaCl \cdot 2H_2O$, does not crystallize until the ice temperature is $-23°C$, which is lower than any ice temperature we observed. Additionally, if the flowers were indeed salt crystals, then their salinity would be 1000 ppt. Though the surface crystals were indeed quite salty, observed salinities were only as high as 110 ppt, confirming that they were ice crystals with entrained brine.

If frost flowers result from ice growth from the vapor phase, what is the source of the vapor? Measured relative humidities during LEADEX were in the 85–95% range (D. Wolfe, personal communication, 1993) and were consistent with the finding of earlier researchers [*Malmgren*, 1927] that springtime relative humidities are often near saturation. An obvious candidate for the necessary added source is the open lead with its associated tremendous fluxes of water vapor to the atmosphere. If the lead was the sole source of added vapor, one would expect frost flowers to be ubiquitous and appear on the adjacent, thicker sea ice as well as the lead ice. However, in all the cases we observed, there was an abrupt end to the frost flowers at the edge of the lead, and none were observed on the adjacent thicker sea ice or on any equipment installed in or near the lead. This suggests that while the water vapor from open water may contribute to creating the conditions necessary for frost flowers, it alone is not always sufficient.

Two components that appear critical in the formation of frost flowers on lead ice are the surface brine skim and the raised ice surfaces or bumps that we suggest develop above this skim as a result of brine expulsion. The surface skim is a source of additional water vapor, allowing for supersaturation locally over the lead ice. The bumps serve as nucleation sites for the frost flowers. This would account for our observation that the frost flowers do not cover the sea ice uniformly, but rather are discrete clumps of ice. Also, in the absence of this small-scale topography the brine skim would form a continuous slurry of brine and frazil ice, prohibiting the growth of frost flowers. Differences in the saturation vapor pressure are generated from variations in the temperature and composition between the bumps of ice and the surface skim. This serves as a driving mechanism for the transfer of vapor from the liquid, warmer surface of the brine to the solid, colder surface of the ice and results in the formation of frost flowers. As the frost flowers develop, the local topography is enhanced, providing the potential for positive feedback in frost flower growth.

To evaluate this proposed mechanism, we shall compare an estimate of the observed frost flower mass to a theoretically predicted value. At lead 4 in the main experiment we were able to observe frost flower development over a 2-day period, monitoring the frost flowers' fabric, areal coverage, and height, as well as air, ice, and brine skim temperatures. Because of their extremely delicate nature it was impossible to directly measure the mass of the frost flowers. However, we were able to determine that they were roughly 1.5 cm high and covered about one third of the surface area and that the bulk density of the frost flower layer was comparable to that of fluffy new snow, approximately 0.05–0.10 g cm^{-3}. From these observations we estimate that the mass per unit area of the frost flowers was 0.025–0.050 g cm^{-2}.

Calculation of an estimated mass flux is made by following the lead of *Colbeck* [1988] and assuming that diffusion alone is too slow a process to generate the observed frost flowers and that virtually all of the growth is due to turbulent mixing, giving

$$dm/dt = Cu\Delta\rho \quad (2)$$

where m is the mass, C is the exchange coefficient, u is the wind speed, and $\Delta\rho$ is the vapor density difference between the brine skim and the elevated ice where the flowers formed. A value of 2.1×10^{-3} was used for the exchange coefficient [*Andreas*, 1987], and a wind speed of 1 m s^{-1} was assumed. The vapor density (ρ_v) can be expressed as a vapor pressure using the perfect gas law [*Wallace and Hobbs*, 1977],

$$\rho_{vi,vw} = 100e_{vi,vw}/R_vT$$

where i refers to ice, w refers to water, e_v is the vapor pressure in millibars, T is temperature in degrees Kelvin, and R_v is the gas constant for 1 kg of water (461 J deg^{-1} kg^{-1}). Assuming that the air above the brine and ice is saturated, and ignoring any geometrical effects, the saturation vapor pressure is computed using relations for moist air from *Buck* [1981] above water (e_w) and ice (e_i),

$$e_w = [1.0007 + 3.46 \times 10^{-6}P] \cdot \left[6.1121 \times \exp\left(\frac{17.966T}{247.15 + T}\right)\right]$$

$$e_i = [1.0003 + 4.18 \times 10^{-6}P] \cdot \left[6.1115 \times \exp\left(\frac{22.452T}{272.55 + T}\right)\right]$$

where P is the atmospheric pressure in millibars and T is the temperature. Since the surface skim is not pure water, but has a high concentration of salts, the saturation vapor pressure is corrected using [*Sverdrup et al.*, 1942]

$$e'_b = e'_w(1 - 0.000537S_b)$$

where S_b is the surface skim salinity in parts per trillion. Equation (2) was evaluated at discrete times using measured brine skim and air temperatures and then was numerically integrated over time to generate the cumulative mass transport. The measured temperatures and the calculated cumulative mass transport are plotted in Figure 6. Air temperatures were typically 5° to 10°C lower than the brine skim temperatures. The largest predicted mass fluxes occurred in the early stages when the brine skim was relatively warm and its water vapor density was a maximum. Final values of the mass per unit area of frost flowers after 2 days of growth were 0.030 g cm^{-2}, comparable to the observed values. This analysis therefore supports the possibility that the brine skim provides the source of surplus water vapor needed for the growth of frost flowers.

This mechanism does differ somewhat from the characteristic way surface hoar is produced. Surface hoar typically forms on calm nights when, because of radiation cooling, the surface temperature falls below that of the air, resulting in supersaturation and subsequently sublimation [*Seligman*, 1936; *Lang et al.*, 1984; *Colbeck*, 1988]. In our case the driving force is the difference in saturation vapor pressure between brine and ice. Another difference in the frost flower case is that the surface, i.e., the brine skim, is warmer than both the air and the surface ice bumps, making radiational cooling less of a factor.

As we have described, the frost flowers are initially fresh ice features. How, then, do they develop their high salinity? There is little doubt that the source of the salts is the highly saline surface skim that lies at the base of the flowers. The mechanism responsible for the transport of the brine from the surface up into the frost flowers is not as clear. On the basis of our salinity measurements, however, we know that salts at a concentration of approximately 0.070 g cm^{-3} of water were present at the top of the 15-mm-high frost flowers 12 hours after they began to form. Given this rapid salination of the frost flowers, the most likely mechanism for the transport of brine into the frost flowers, and one that has been suggested by other researchers [*Drinkwater and Crocker*, 1988], is surface tension. Studies examining the microstructure of frost flowers and the distribution of brine with frost flowers are needed to test the surface tension hypothesis.

Conclusions

Observations indicate that the surface characteristics of lead ice change significantly during the early growth phase.

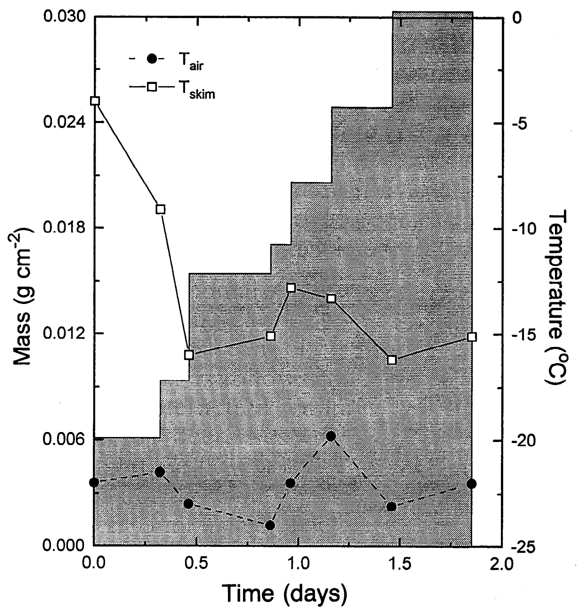

Figure 6. The cumulative mass transport, the air temperature, and the brine skim temperature plotted as a function of time.

These changes affect the roughness, salinity, and brine volume of the surface of the sea ice and, therefore, have a major impact on the microwave signature. Under quiescent conditions a sea ice cover begins to form almost immediately after the lead opens. Initially, the ice surface is smooth and dry. Once the sea ice cover reaches a thickness of 1 to 2 cm, a thin layer of highly saline brine appears on the surface. This brine skim plays a critical and multifaceted role in the evolution of sea ice surface conditions. As the surface brine skim cools, it becomes a slurry of ice and brine. The once smooth surface develops small-scale topography characterized by protuberances of ice rising above the brine skim. These ice bumps may serve as nucleation sites for frost flowers, a form of surface hoar. In the cases observed, we believe that the brine skim further contributed to frost flower development by providing a source of surplus water vapor necessary for their growth. The crystal structure of the frost flowers varies, depending primarily on the air temperature during formation. The initially fresh frost flowers quickly become salty as the brine from the surface skim is "wicked up" into the frost flowers due to the effects of surface tension. This results in a high brine volume for individual frost flowers. If the frost flowers are considered as a layer, however, because of their low bulk density, the total brine content of the flowers is small relative to the surface skim and the upper portion of the sea ice.

In this paper we have presented observations of lead ice surface conditions during the first few days of ice growth and speculated as to possible underlying physical mechanisms. While estimates of brine and water vapor fluxes support the proposed mechanisms for the formation of the surface skim, development of frost flowers, and the entrainment of brine in frost flowers, additional research is needed. Because of the intricate nature of the problems and the difficulty in performing lead field experiments, laboratory studies are a particularly appropriate approach to these issues. Areas of particular interest include a closer examination of the origin of the surface brine skim, the formation of surface roughness bumps and their role in frost flower formation, a statistical description of the evolution of surface roughness, a determination of the spatial distribution of brine on frost flowers, and further investigation of the role of the brine skim as a water vapor source in frost flower growth. An improved understanding of the specific processes involved in the development and temporal variations of the surface characteristics will permit us to more accurately assess their impact on the electromagnetic properties of sea ice.

Acknowledgments. This work was funded by the Office of Naval Research under the leads initiative. The authors thank S. Ackley, S. Colbeck, M. Sturm, W. Tucker, and two anonymous reviewers for their helpful and insightful comments. Particular thanks go to J. Wettlaufer for helpful and insightful discussions regarding the physics pertinent to this problem.

References

Andreas, E. L, A theory for the scalar roughness and the scalar transfer coefficients over snow and sea ice, *Boundary Layer Meteorol.*, *38*, 159–184, 1987.

Buck, A. L., New equations for computing vapor pressure and enhancement factor, *J. Appl. Meteorol.*, *20*, 1527–1532, 1981.

Colbeck, S., On the micrometeorology of surface hoar growth on snow in mountainous areas, *Boundary Layer Meteorol.*, *44*, 1–12, 1988.

Cox, G. F. N., and W. F. Weeks, Brine drainage and initial salt entrapment in sodium chloride ice, *Res. Rep. 345*, 85 pp., Cold Reg. Res. and Eng. Lab., Hanover, N. H., 1975.

Cox, G. F. N., and W. F. Weeks, Equations for determining the gas and brine volumes in sea ice samples, *J. Glaciol.*, *29*, 306–316, 1983.

Crocker, G. B., and J. E. Lewis, Some physical properties of snowcover on evolving first year sea ice, paper presented at 42nd Eastern Snow Conference, Montreal, Quebec, Canada, June 6 and 7, 1985.

Drinkwater, M. R., and G. B. Crocker, Modelling changes in the dielectric and scattering properties of young snow-covered sea ice at GHz frequencies, *J. Glaciol.*, *34*, 274–282, 1988.

Gow, A. J., W. B. Tucker III, and W. F. Weeks, Physical properties of sea ice in the Fram Strait, June–July 1994, *Rep. 87-16*, U.S. Army Cold Reg. Res. and Eng. Lab., Hanover, N. H., 1987.

Grenfell, T. C., and J. C. Comiso, Multifrequency passive microwave observations of first-year sea ice grown in a tank, *IEEE Trans. Geosci. Remote Sens.*, *GE-24*, 826–831, 1986.

Grenfell, T. C., D. J. Cavalieri, J. C. Comiso, M. R. Drinkwater, R. G. Onstott, I. Rubinstein, K. Steffen, and D. P. Winebrenner, Considerations for microwave remote sensing of thin sea ice, in *Microwave Remote Sensing of Sea Ice*, *Geophys. Monogr. Ser.*, vol. 68, edited by F. D. Carsey, pp. 291–301, AGU, Washington, D. C., 1993.

Hobbs, P. V., *Ice Physics*, 837 pp., Clarendon, Oxford, 1974.

Kobayashi, T., The growth of snow crystals at low supersaturations, *Philos. Mag.*, *6*, 1363–1370, 1961.

Lang, R. M., B. R. Leo, and R. L. Brown, Observations on the growth processes and strength characteristics of surface hoar, paper presented at International Snow Science Workshop, Mt. Rescue-Aspen, Aspen, Colo., Oct. 24–27, 1984.

LEADEX Group, The LEADEX Experiment, *Eos Trans. AGU*, *74*, 393, 396–397, 1993.

Magono, C., and C. W. Lee, Meteorological classification of natural snow crystals, *J. Fac. Sci. Hokkaido Univ.*, *Ser. VII*, *2*, 321–335, 1966.

Malmgren, F., Studies of humidity and hoar-frost over the Arctic Ocean, *Geofys. Publ.*, *4*, 3–19, 1927.

Maykut, G. A., Large-scale heat exchange over young sea ice in the central Arctic, *J. Geophys. Res.*, *87*, 7971–7984, 1982.

Nakaya, U., *Snow Crystal, Natural and Artificial*, 76 pp., Harvard University Press, Cambridge, Mass., 1954.

Ono, N., and T. Kasai, Surface layer salinity of young sea ice, *Ann. Glaciol.*, *6*, 298–299, 1985.

Onstott, R., SAR and scatterometer signatures of sea ice, in *Microwave Remote Sensing of Sea Ice*, *Geophys. Monogr. Ser.*, vol. 68, edited by F. D. Carsey, pp. 73–104, AGU, Washington, D. C., 1993.

Seligman, G., *Snow Structure and Ski Fields*, 555 pp., Macmillan, New York, 1936.

Sverdrup, H. U., M. W. Johnson, and R. H. Fleming, *The Oceans*, 1087 pp., Prentice-Hall, Englewood Cliffs, N. J., 1942.

Tucker, W. B., J. A. Richter-Menge, and A. J. Gow, Variations in mechanical properties within a multi-year ice floe, paper presented at *OCEANS '89*, Inst. of Electr. and Electron. Eng., Seattle, Wash., Sept. 19–21, 1989.

Untersteiner, N., Natural desalination and equilibrium salinity profile of perennial sea ice, *J. Geophys. Res.*, *73*, 1251–1257, 1968.

Wallace, J. M., and P. V. Hobbs, *Atmospheric Science: An Introductory Survey*, 467 pp., Academic, San Diego, Calif., 1977.

Weeks, W. F., and S. F. Ackley, The growth, structure, and properties of sea ice, *CRREL Monogr. 82-1*, 130 pp., Cold Reg. Res. and Eng. Lab., Hanover, N. H., 1982.

Wensnahan, M. R., T. C. Grenfell, D. P. Winebrenner, and G. A. Maykut, Observations and theoretical studies of microwave emission from thin saline ice, *J. Geophys. Res.*, *98*, 8531–8545, 1993.

D. K. Perovich and J. A. Richter-Menge, U.S. Army Cold Regions Research and Engineering Laboratory, 72 Lyme Road, Hanover, NH 03755.

(Received July 12, 1993; revised April 8, 1994;
accepted April 22, 1994.)